Landslides
DOI 10.1007/s10346-020-01427-1
Received: 15 October 2019
Accepted: 5 May 2020

Giona Preisig

Forecasting the long-term activity of deep-seated landslides via groundwater flow and slope stability modelling

Abstract Large (deep-seated) landslides present complex geometries, rock/soil properties, and kinematical behavior. Complex geometries are due to the presence of several sliding zones, while complex properties typically result from the dilation, compression, or fatigue of geologic materials. Kinematical behavior is often episodic, with periods of stability followed by periods of enhanced slope movements owing to shear strength reduction in response to groundwater pressure changes. These mechanisms complicate our capacity in forecasting the long-term activity and thus, the choice of a strategy for hazard management. This technical note introduces a method for predicting the long-term activity of deep-seated landslides based on one-way coupled hydromechanical numerical modelling. The method is applied to analyse the long-term stability of a deep-seated compound slide in the Swiss Jura Mountains. Results indicate that, under natural groundwater pressure changes, the analysed compound slide will continue to move in an episodic fashion in response to groundwater levels in the slope, without developing velocities greater than several centimeters per year. This example demonstrates how one-way coupled hydromechanical modelling constrained by field data is a reliable tool for assessing the long-term activity of deep-seated landslides and helping the management of associated hazards.

Keywords Long-term forecasting · Hydromechanical modelling · Slope hydrogeology · Deep-seated compound slides · Swiss Jura Mountains

Introduction

Forecasting the short- and long-term activity of landslide phenomena is recognized as one of the most challenging tasks in geological engineering. This is mainly because failure processes, e.g., progressive failure accompanying creep, are enhanced or inhibited by weakening or strengthening phenomena, such as groundwater pressure changes, freezing, or loss/gain of material strength. Indeed, rock and soil properties, along with hydrogeologic conditions, always present specific spatial characteristics that might change with deformation. This implies that each natural soil or rock slope on Earth will behave differently to triggering mechanisms, depending on its intrinsic characteristics and deformation history (Crosta and Agliardi 2003; Hungr et al. 2014; Eberhardt et al. 2016). The observational method through geologic, geotechnical, hydrogeologic, and geophysical field studies is the most efficient approach for predicting the short- and long-term activity of landslides. This allows a systematic classification of the landslide type according to a well-established approach, e.g., the updated Varnes classification of landslide types (Hungr et al. 2014). Long-term activity, that is months to decades, is then forecasted by making parallelism with landslides of the same type and synthetizing the information in natural hazard maps, which are a basis for land use planning (Lateltin et al. 2005). Short-term predictions, covering response times from seconds to days, can be tackled at the local scale by systems monitoring deformation rates coupled with early warning devices (Leonard et al. 2013). In the case of rock collapses, processing and interpreting measured deformation rates via Fukuzono's (1985) inverse velocity method might lead to reliable forecasts a couple of days prior to the ultimate failure (Loew et al. 2017). However, many examples exist where deep-seated landslides have accelerated to alarming levels and then returned to base rates of displacement, for example, the Moosfluh slide, in Valais, Switzerland (Strozzi et al. 2010; Grämiger et al. 2017), or the La Clapière slide in the Maritime Alps, France (Hungr and Evans 2004). At large scales, short-term predictions can be tackled also by predictive tools based on weather forecasts (Leonarduzzi et al. 2017). Nevertheless, these are specific to shallow slides, and their reliability is only valid for regional applications, such as national alert programs.

When calibrated against field data and observations, limit equilibrium methods and/or numerical models of slope activity give detailed information on slide kinematics and triggering processes. They can further be used for forecasting slide behavior and designing or verifying mitigation measures (Vuillet and Hutter 1988; Eberhardt et al. 2004; Tacher et al. 2005; Hendry et al. 2015). Numerical modelling of slope activity typically implies first, a detailed simulation of the dominant destabilizing processes, such as groundwater flow (Preisig et al. 2016; Kukemilks et al. 2018) and/or seismic loading (Gischig et al. 2016), and second, the simulation of the kinematical response.

This technical note aims to present a modelling procedure for forecasting the long-term activity of deep-seated landslides based on one-way coupled hydromechanical numerical models. The approach is described in the next section and then applied to a case study, that is Les Buges slide, a clay/rock compound slide located in the Swiss Jura Mountains (Preisig 2018; De Boni 2018).

Method description

Background and applicability of the modelling procedure

The deformation history of a landslide includes different stages of activity (Leroueil et al. 1996; Pánek and Klimeš 2016). Each stage needs a distinct model.

Debuttressing in response to glacial melt or fluvial erosion in the lower slide part is often at the origin of *first-time failures* of natural slopes. These led to the development of fully-connected sliding zones where rock and soil strength reduced from peak to residual and changed the natural slope in a deep-seated landslide (DSL) in which promoting forces are close to resisting forces. This is a state of limiting equilibrium where the slope *factor of safety* (*FoS*) is equal to unity (Hungr et al. 2014). This *first stage* can be very rapid relative to geologic times ($< 10^2$ years).

Published online: 26 May 2020

The *second stage* of the slide's deformation history includes *post-failures and re-activation phases*. If the geometry and boundary conditions of an active DSL are still representative of those arisen after first-time failures and are well-characterized by field studies, then residual strength properties of rock and soil forming the principal sliding zones and characterizing the *post-failure state*, can be back-calculated by means of a numerical model solving for a *FoS* of unity. This is implemented in a numerical model via a strength reduction procedure, i.e., the progressive reduction of shear strength properties until reaching a state of limiting equilibrium: $FoS = 1$ (Dawson et al. 1999). This computation corresponds to *Step 1* of the proposed modelling procedure, and it is applicable to DSL where the morphology did not change substantially during the second stage and where the formation of sliding zones is related to gravitational mechanisms. The model geometry is thus based on the present-day topography (Table 1).

Episodic *re-activation phases* occur due to changing effective stresses owing to external triggers, such as important seismic loading or significant groundwater recharge. This stage can be extremely long, e.g., > 10^3–10^4 years for deep-seated landslides, implying for numerical modelling a simplification of governing equations. In the case of hydromechanical interactions, simplification is realized by first calculating groundwater pressure distributions in the slide via a groundwater flow model, and then introducing them into a slope stability model for simulating the kinematical response (Tacher et al. 2005; Preisig et al. 2016). The target of *Step 2* is thus to verify if under the external trigger, in our case groundwater pressure changes, modelled displacements match observed data by using rock and soil properties back-calculated in *Step 1* (Table 1). The aforementioned simplification reduces the hydromechanical interaction to a one-way coupled process, as we neglect changes in pore pressure due to stress modifications and consider constant hydrogeologic properties. The first point limits the application of the modelling procedure to the common situation where pore pressure changes are associated to varying conditions of groundwater recharge. The second point, i.e., assumption of constant hydrogeologic properties, limits the numerical model to a time window of some decades. This is principally because for larger time-scales (> 10^2 years), deformation might become large enough to change hydrogeologic properties (Pánek and Klimeš 2016; Preisig et al. 2016; Preisig 2018). However, field data of landslide monitoring rarely exceed some decades of observation and can thus be used to achieve the goal of *Step 2*.

The deformation history ends either by a full or partial *self-stabilization*, or else by a rapid and sudden, *ultimate failure* (hours to days) of a large part of the slide (*third stage*). Deep-seated compound slides are more prone to self-stabilizing, as the basal sliding zone often presents a curvature or is gently dipping, compared to collapse slides, which are more disposed to accelerate into a complex, ultimate failure. *Step 3* targets thus predictive calculations for forecasting the long-term behavior of the deep-seated landslide based on information collected during *Steps 1* and *2*. Potential failure processes are tested during *Step 3* (Table 1) and typically include (i) changing hydrogeologic conditions, e.g., effects of climate change or anthropogenic activities (dam

Table 1 Conceptual model of the deformation history of a deep-seated landslide and implications for the modelling procedure

	Stage	1. First-time failure	2. Post-failure and re-activation phases		3. Ultimate failure
Deformation history	**Duration**	< 10^2 years	> 10^3 - 10^4 years		< 10^2 years
	Possible de-stabilizing process	Kinematic debuttressing, e.g., glacial/fluvial erosion at foot of slope	*i)* External physical (e.g. groundwater pressure fluctuations, seismic forcing, thermal stress variations, erosion, etc.) and/or *ii)* anthropogenic factors		*i)* Sudden external physical and/or anthropogenic trigger ; *ii)* progressive weakening of internal material
	Changes in the factor of safety *FoS* (according to Popescu 1994)	From *stable* (*FoS* > 1) to *marginally stable* (*FoS* ≈ 1)	*Marginally stable* (*FoS* ≈ 1)		From *marginally stable* (*FoS* ≈ 1) to *actively unstable* (*FoS* < 1 if failure)
	Slope deformation and typical velocity	Significant > 1-10 cm day^{-1}	Moderate < 2-200 cm year^{-1}		Significant > 1 cm hour^{-1}
Implications for the modelling procedure	**Modelled slope geometry**	Based on the *pre-first-time failure topography*	Based on the *present-day topography*		
	Modelled strength properties of rocks/soils	*Peak* shear strengths	*i)* Sliding zones: *residual* shear strengths *ii)* Sliding masses: *mobilized* shear strengths		*i)* Sliding zones: *residual* *ii)* Sliding masses: *further weakening*
	Modelling step	Not modelled	***Step 1***	***Step 2***	***Step 3***
	Scope		*Back-calculation* of strength properties	*Verification* of the external trigger (in this study: groundwater pressure changes)	Test potential failure processes and *forecast* the long-term activity
	Type of numerical models		*Slope stability*: strength reduction method	*Groundwater (*GW*) flow* & *slope stability* (one-way coupled HM analyses)	
	Calibration strategy		*FoS* = 1	Modelled external trigger (GW pressure changes) and displacements match field data	-
	Assumptions and limitations		*i) FoS* = 1 *ii)* Geometry and boundary conditions are known *iii)* Gravitational kinematics	*i)* GW pressure changes due to varying recharge *ii)* No GW pressure changes due to stress changes *iii)* Constant hydrogeologic properties during the observational period	*i)* As in *Step 2* *ii)* Predictive calculations valid/limited to some decades due to the assumption of constant hydrogeologic properties
	Possible ultimate failure triggers		-	-	*i)* Changing hydrogeologic conditions *ii)* Changing mechanical conditions, e.g., erosion *iii)* Changing material properties of the sliding mass (progressive weakening)

construction) on groundwater pressure variations; (ii) changing mechanical conditions, e.g., effects of enhanced fluvial erosion or anthropogenic excavations at the slide's toe; or (iii) changing rock and soil properties, e.g., progressive loss of mobilized shear strengths of the sliding mass or rock blocks due to material fatigue. Note that due to the assumption of constant hydrogeologic properties, predictive calculations are limited to a time window of some decades from the period of site characterization.

Computer software

The finite element software FeFlow (Mike DHI 2018) is used to model groundwater flow and pore pressure changes, while the geotechnical software FLAC (Itasca 2018) is used to analyze landslide response to varying hydrogeologic conditions and other triggering mechanisms. The strength reduction technique is automatized in FLAC, which simplifies the realization of *Step 1* of the modelling procedure: back-calculation of soil and rock properties by imposing a factor of safety $FoS = 1$. For *Steps 2* and *3*, a routine written in FISH, the internal programming language of FLAC, allows the interaction between FeFlow and FLAC. Outputs from hydrogeologic modelling consist of a series of ASCII files. Each file contains a modelled distribution of groundwater pressure for a given season at the nodes of the finite element mesh. The series of files covers several years of groundwater pressure changes owing to seasonal variations. In FLAC, after the initialization of the in situ stress field, the FISH routine (i) reads groundwater pressures of the first season, (ii) interpolates them to the finite difference grid, (iii) simulates the state of the landslide that is the kinematical response to pressure changes, and (iv) repeats the procedure for all distributions (seasons) in the series. 10'000 calculation steps are accomplished by FLAC in point (iii) to model a new state of the landslide in terms of stresses and displacements. If the modelled slope undergoes a large failure, simulated displacements do not stabilize during the calculation steps and become unrealistic. In such a case, the simulation is stopped; otherwise, the next hydrogeologic state is applied, and the routine goes on.

Hydromechanical formulation, material properties, and constitutive models

The principal advantage of a one-way coupled hydromechanical model is that groundwater flow and slope stability are calculated separately. This simplification allows numerical analyses at the spatial (km) and temporal (decades) scales required by deep-seated landslides. Hydrogeologic and geomechanical processes are coupled via the Terzaghi definition of effective stress. Changing pore pressure distributions are calculated a priori by solving the groundwater flow equation under varying conditions of hydrogeologic recharge, e.g., low versus high water levels. These distributions are then applied to update effective stresses and calculate a new landslide state by solving for a stability criterion, e.g., Mohr-Coulomb. Any change in groundwater pressure within the landslide implies a reduction or an increase in resisting forces and thus, a new state of stability.

Step 1 targets the back-calculation of material properties constituting the landslide. For rocks/soils forming the principal sliding zones, this step gives their residual strength values. For cohesion, this means a state of cohesionless (or close to) due to the large deformation occurred during first-time failures. For rocks/soils forming the sliding mass, this step gives their mobilized shear strengths (Table 1). Obtained residual values for the principal sliding zones are then used in *Steps 2* and *3*. The modelling of further weakening is thus no more possible for these zones. For geologic materials forming the sliding mass, further weakening might be considered in *Steps 2* and *3* due to on-going fatigue or weathering processes that decrease progressively the mobilized shear strength. This is implemented in the modelling procedure by applying an elasto-plastic formulation with strain softening. One behavioral law is the Mohr-Coulomb model with strain softening, which allows for nonlinear material softening from peak/mobilized to residual strength properties with increasing plastic strain. Other laws exist and might be applied depending on the conceptual model of the landslide and the objectives of the numerical study. Note also that in *Steps 2* and *3*, at least two hydrogeologic states per year have to be modelled for mimicking the seasonal change of groundwater pressures.

Les Buges slide

Generalities

The Les Buges deep-seated compound slide is located in the Swiss Jura Mountains, in Boudry (Canton Neuchâtel), on the north slope of the Areuse River in a forest environment. The slide is about 1.1-km wide and 400-m long for a volume of about 9 million m^3. The depth of the basal sliding zone increases from west, where it is about 10-m deep, to east, where it exceeds more than 60-m depth (Preisig 2018). Various infrastructures at risk, among others a regional railway line, a powerline, and an aqueduct, are periodically damaged by the slow slope movement or related natural hazards: rock falls, topples, and debris slides. In the '80s, the main concern of governmental authorities was a catastrophic scenario, where failure of Les Buges slide would cause the formation of a dam-lake in the Areuse gorges and a hazard of lake outburst with debris floods (Meia 1996).

Slide geology, hydrogeology, and kinematics

In the *west body* (Fig. 1), Les Buges is a rock-clay compound slide characterized by a rotational movement along two main horizons of weakness: at the bottom of Hauterivian marls and at the bottom of Quaternary deposits, where a silty clay layer is present (Fig. 2b). These two horizons of low strength are interbedded with at least three permeable strata: a perched aquifer in silty sand and gravel layers of the Quaternary deposits near the silty clay horizon, a conductive layer of small to middle permeability in the Hauterivian marls, and, at the bottom, a karstic system in c_{1P} Berriasian limestones (Fig. 2b). Springs at the toe of the Quaternary aquifer, i.e., Trois Rods springs, were used for water supply. The watershed of the karstic system largely exceeds the slide extent; nevertheless, this system is too deep to interact with the sliding zone (De Boni 2018; Preisig 2018). Figure 1 schematizes slide movement velocities: in the *west body*; velocities are higher and increase downslope due to the presence of the Quaternary soil deposits and because of shear strength reduction in response to the seasonal change of groundwater pressure, in both aquifer and aquitard layers. The temporal evolution of the flow rate measured at the Trois Rods springs is a clear proxy of the seasonal change of groundwater pressure with maximum values typically observed during the winter–spring period (flow rate > 15 L/min), when water infiltration is favored by vegetation at nil levels of activity (Fig. 2a). During this period, slide velocities in the lower part of the *west body* are seen to increase from

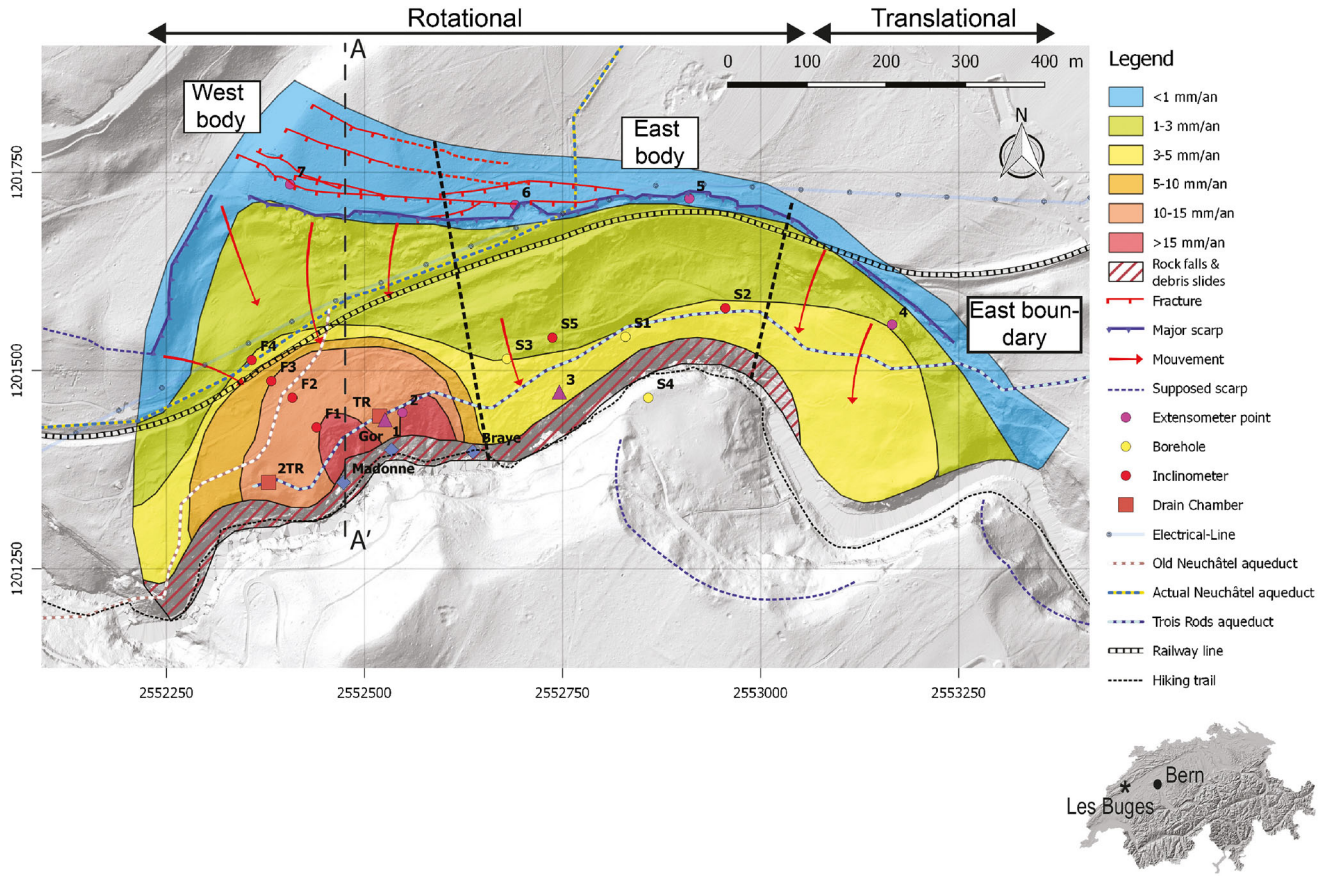

Fig. 1 Map summarizing landslide velocities, geomorphologic features, observation points, and infrastructures at risk at Les Buges deep-seated compound slide (modified after De Boni 2018 and Preisig 2018)

base velocities of a couple millimeters per year to peak velocities of several centimeters per year (Fig. 2c).

In the *east body*, the Quaternary cover is lacking. Herein, Les Buges is a rock compound slide characterized by a movement along a very thin zone (< 1 m thick) of uneven curvature situated at the bottom of the Hauterivian marls (Fig. 2b). Rotational movement dominates and is observed in the lower slide part by the presence of rock blocks with dip of bedding planes reversed compared to the regional dip, i.e., 15–20° SE. Yet, close to the east slide boundary, movement is translational. Velocities are extremely slow in the *east body*, i.e., millimeter per year (Fig. 1), governed by the slope creep. The slide hydrogeology is quite different, with only the conductive layer of middle to small permeability in the Hauterivian marls producing a seepage zone at the slide's toe. Increasing groundwater pressures during the winter—early spring period is inhibited in the *east body* by (i) in the upper slide part, tension cracks behaving as preferential flow paths and by-passing infiltrated waters to the karstic system at-depth, in the c_{1P} Berriasian limestones (Fig. 1); and (ii) in the lower slide part, a highly damaged and dilated rock mass favoring rapid drainage and avoiding the rise of overpressures (Preisig 2018).

Numerical analysis for predicting long-term landslide activity

We analyze the long-term activity of Les Buges by applying the modelling procedure introduced before. Field observations indicate that a 2D vertical cross section along the *west slide body* from north to south permits us to analyze the most critical part of the landslide: section A-A′ in Fig. 1, and the hydrogeologic seasonality can be simplified in two dominant states: low (June to November) and high (December to May) groundwater pressures (Fig. 2a). As reported above, the *east slide body* is controlled by a different kinematic compared to the *west body* and will need a different modelling approach. The choice of modelling the *west body* in 2D is justified by a velocity field more or less regular in terms of spatial distribution (Fig. 1) and because the slide geometry is well constrained in 2D by field data. The construction of the geometry and shear zones of the slide in 3D will integrate more uncertainty due to the lack of field data. This will result in a decrease of model reliability. According to Leroueil et al. (1996), the slide is in the reactivation stage with soil and rock properties of the sliding zones at residual values and a factor of safety approaching the unity. The *west body* moves at rates mostly controlled by groundwater pressure changes. The *first step* of the model targets back-calculating residual strength properties of the sliding zones by constraining a slope factor of safety of unity under high groundwater pressures. The *second step* aims to verify if observed displacements are correctly reproduced under groundwater pressure changes. For this, a seasonal state of groundwater pressure (low and high) was first modelled in *FeFlow* for the period 1980–2018 based on (effective) precipitation data. The *third step* targets to forecast the long-term landslide activity by testing two scenarios of possible failure mechanisms: (i) changing infiltration rates according to precipitation trends as predicted by climate change scenarios for Western Switzerland (CH2018 2018) and (ii) a progressive loss of the mobilized shear strength of the sliding mass.

Model geometry and implemented geologic heterogeneity

Figure 3 presents the model geometry with the heterogeneity of soil and rock properties. The domain is a 600-m long and 150-m high 2D vertical section through the *west slide body*. This section is representative for the most critical sector of the *west body*, which is about 50-m wide in the 3rd dimension. Slide geometries and geologic heterogeneity of soil and rock properties are constrained by superficial observations (geologic map), lithological description of boreholes, and geophysical data (De Boni 2018; Preisig 2018).

Boundary conditions, settings, and calibration strategy for the groundwater flow model

Boundary conditions for the groundwater flow model include an imposed recharge, i.e., fluid-fluxes mimicking infiltration rates, in the upper and middle slide part (pink crosses in Fig. 3a) and a seepage condition in the lower slide part (blue circles in Fig. 3a). The seepage condition stands for a hydraulic head matching atmospheric pressure, that is, water pressure is zero, and the hydraulic head matches the elevation potential (node altitude). The extent of the seepage condition is based on field observations and mimics the drainage at the slide's toe due to the presence of water catchments (Trois Rods springs). Seasonal infiltration rates have been computed based on precipitation and snow melt data from 1980 to 2018 (MeteoSwiss 2018), as well as infiltration conditions at Les Buges according to Preisig (2018). Infiltration is typically 20% of the precipitation in the summer period, while it approaches 60 to 70% in the winter period due to vegetation and evaporation at nil levels of activity.

The groundwater flow model has been calibrated by varying the hydraulic conductivity of geologic units so that seasonal simulated flow rates in the seepage zone are in good agreement with measured flow rates in the period 2016–2018 (Fig. 2a). Then, seasonal hydrogeologic states for the slide have been simulated for the period 1980 to 2018 by imposing a seasonal change of infiltration rates.

Boundary conditions, constitutive models, and initial in situ stress field for the slope stability model

Figure 3b illustrates boundary conditions, geologic heterogeneity, and location of observation points in the slope stability model. Boundary conditions of fixed zero normal velocity are imposed along the side and bottom boundaries of the model domain. Two

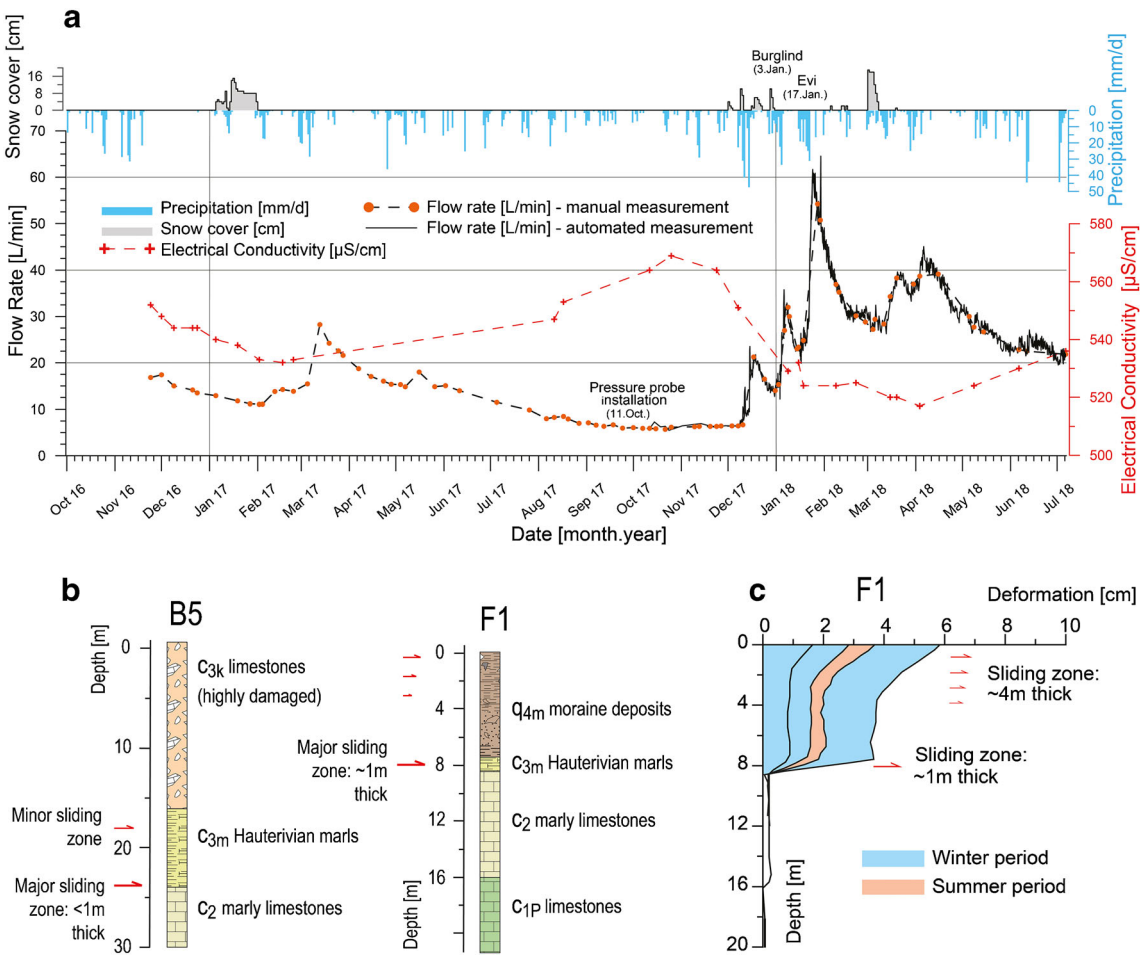

Fig. 2 **a** Flow rate of Trois Rods springs, water electrical conductivity, precipitation, and snow cover measured between autumn 2016 and summer 2018 at Les Buges. Burglind and Evi were two storms that affected Switzerland in early 2018. **b** Lithostratigraphy for the (F1) west and (B5) east slide bodies. **c** Historic cumulative deformation of borehole F1 derived from repeated inclinometer measurements: the seasonal behavior is highlighted by (winter) blue and (summer) orange color (modified after De Boni 2018 and Preisig 2018)

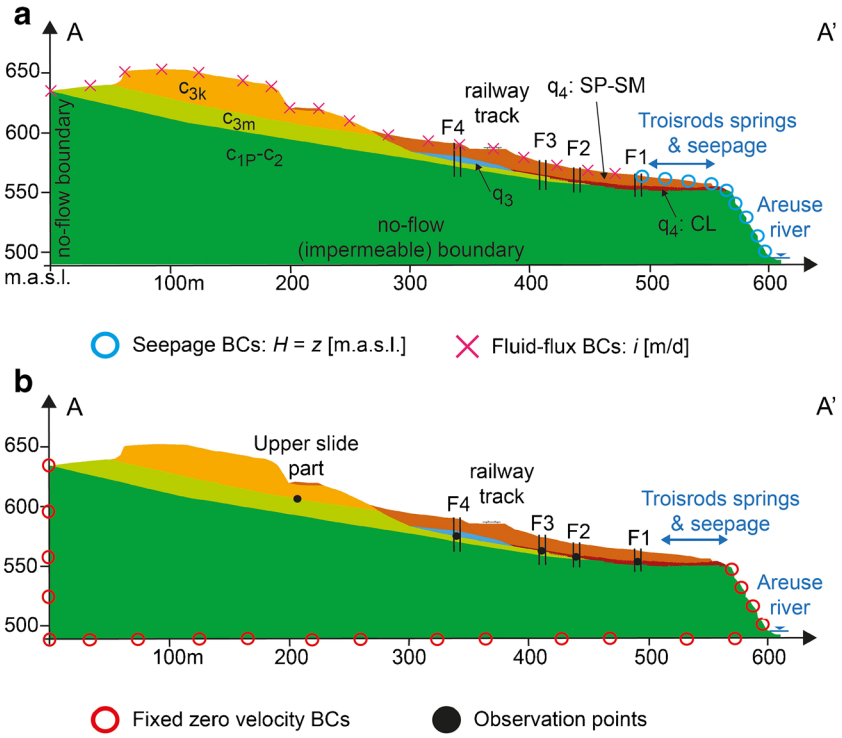

Fig. 3 Geometry, heterogeneity, and boundary conditions (BCs) used in **a** the groundwater flow and **b** slope stability model of the *west slide body*. Refer to Table 2 for the name of geologic units. The finite element mesh for the groundwater flow model is composed of about 100'000 triangular elements (quasi-equilateral) of 1 m edges. The finite difference grid for the slope stability model includes 2172 quadrilateral elements with a refinement at the sliding zone. The size of elements is herein about 3 m large per 1 m height

different constitutive models are considered c_{1P} and c_2 limestones (stable basement) as linear elastic materials, while a Mohr-Coulomb plastic model is used for the remaining geologic units c_{3k}, c_{3m}, q_3, and q_4.

The in situ stress field is initialized prior to the *first step* by solving for gravity loading with the topography and geologic heterogeneity of soil and rock properties as presented in Fig. 3. Parametric inputs for the initialization of the in situ stress field that is specific weight, elastic modulus, and Poisson's ratio are presented in Table 2. Gravity loading leads to a typical mountain-valley configuration of the in situ stress field with a vertical major principal stress and a horizontal minor principal stress in the upper part of the slope, and a horizontal major principal stress and a vertical minor principal stress in the lower part.

Note that for *Steps 2* and *3* of the modelling approach a strain-softening Mohr-Coulomb plastic model was applied to the c_{3k} limestones, as they still weaken with the ongoing deformation and might be at the origin of local collapses, and rock falls in the upper slide part. The strain-softening Mohr-Coulomb plastic model assumes that strength properties soften to residual values, if peak or mobilized shear or tensile strengths are exceeded. In *FLAC*, this requires the specification of peak (or mobilized) and residual strength values, as well as a function specifying the decrease of strength properties with increasing plastic strain. According to the procedure, geologic formations constituting the sliding zones have been considered at a residual state of strength in *Steps 2* and *3*.

Results

Step 1: back-calculated parametric values

Table 2 shows back-calculated values of soil and rock properties from the resolution of *Step 1* and values derived from field and laboratory testing (Routes Nationales Suisses 1996; Preisig 2018; De Boni 2018). For geologic materials constituting the principal sliding zones, c_{3m} marls and q_4–CL deposits, calculated values are residual ones, as shown by the value for cohesion tending to zero. There is a good match between back-calculated values via the modelling procedure and measured data from other studies. The most sensitive properties that govern groundwater flow and the stability of Les Buges compound slide are the hydraulic conductivity, and the friction angle of the clay horizon in the q_4 moraine deposits and the c_{3m} marls. These geologic formations have very low hydraulic conductivity and friction angle and form an impermeable zone of weakness in the slope stratigraphy. This leads to the presence of a perched aquifer in the moraine deposits as shown in Fig. 4a by the zero pressure isoline (white line) and a basal shear zone of irregular curvature. The modelled groundwater flow is quasi-horizontal in the perched aquifer (inset in Fig. 4a).

Step 2: modelled versus observed data

Step 2 considers back-calculated strength properties with sliding zones at residual values and the sliding mass integrating a strain-softening rule. Modelled changes in groundwater pressure between the summer and winter states for the period 1980–2018

Table 2 Values of soil and rock properties (B) back-calculated during *Step 1* and/or (M) measured. SP-SM stands for a poorly sorted sand with silt and gravel and CL for a clay with silt

Geologic unit	Hydraulic conductivity, K [m/s]	Specific weight, γ [kN/m^3]	Elastic modulus, E [MPa]	Poisson's ratio, ν [-]	Cohesion, c [MPa]	Friction angle, ϕ [°]	Tensile strength, T [MPa]	Dilation angle, ψ [°]
q_4 moraine deposits: SP-SM (Sliding mass)	7.0×10^{-6} (M), 1.5×10^{-5} (B)	17 (M), 16 (B)	40–60 (M), 50 (B)	0.4 (B)	0.07–0.12 (M), 0.1 (B_m)	20–30 (M), 25 (B_m)	0.5 (B_m)	1 (B_m)
q_4 moraine deposits: CL (Sliding zone)	1.3×10^{-9} (M), 10^{-9} (B)	18 (M), 16 (B)	40–60 (M), 50 (B)	0.4 (B)	0–0.02 (M), 0 (B_r)	10–20 (M), 8 (B_r)	0 (B_r)	1 (B_r)
q_3 fluvio-glacial deposits (Sliding mass)	10^{-2}–10^{-3} (M), 10^{-3} (B)	18 (B)	60–80 (M), 80 (B)	0.25 (B)	0–0.005 (M), 0 (B_m)	30–40 (M), 32 (B_m)	0 (B_m)	2 (B_m)
c_{3k} limestones (Sliding mass)	10^{-5} (B)	27 (M), 27 (B)	300 (B)	0.3 (B)	5 (B_m), 1 (B_r)	35 (B_m), 30 (B_r)	1 (B_m), 0 (B_r)	3 (B_m)
c_{3m} marls (Sliding zone)	2.4×10^{-8} (M), 2×10^{-8} (B)	22 (M), 22 (B)	100–200 (M), 200 (B)	0.4 (B)	0.005–0.01 (M_r), 0.01 (B_r)	15 (M_r), 12 (B_r)	0 (B_r)	1 (B_r)
c_2 and c_{1P} limestones (Basement)	10^{-6} (B)	27 (B)	300 (B)	0.3 (B)	n/a (elastic)			

(B) denotes values back-calculated during *Step 1* of the modelling procedure. (M) denotes values measured in the field or in the laboratory (after Routes Nationales Suisses (1996), Preisig (2018) and De Boni (2018)). Subscripts (m) and (r) denote mobilized and residual values, respectively

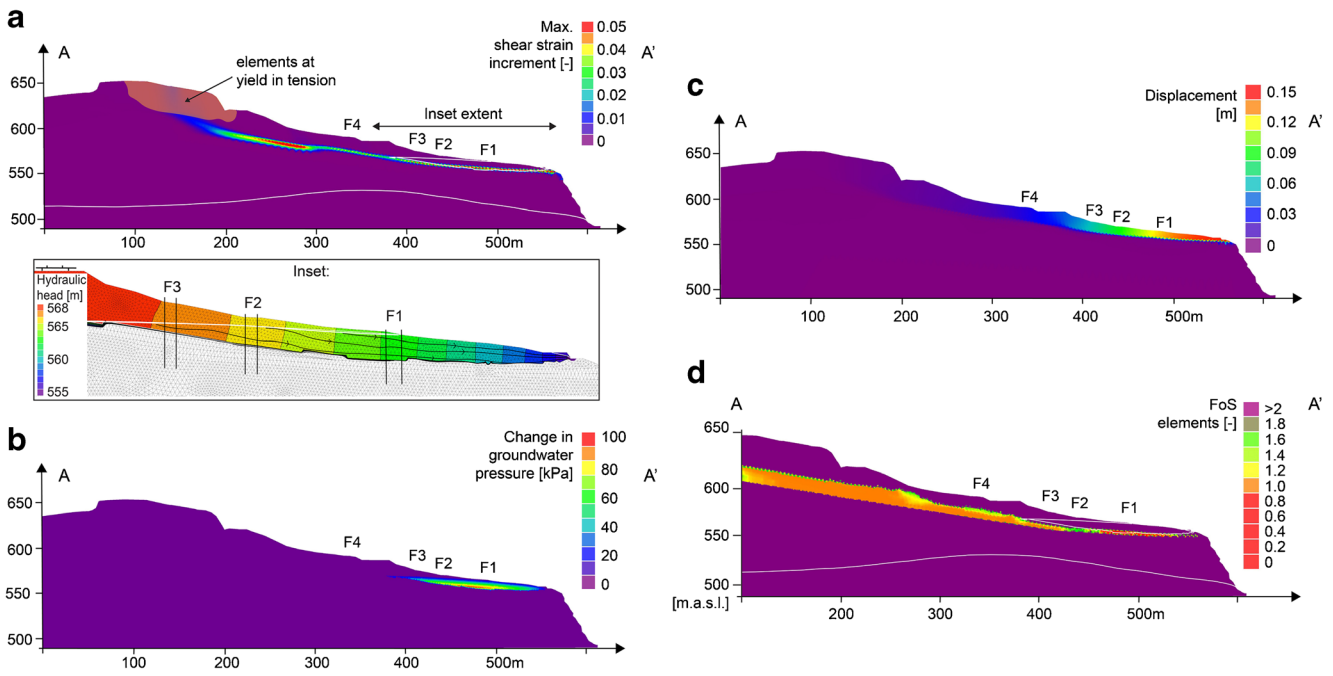

Fig. 4 Model results for *Steps 1* and *2*. **a** *Step 1*, maximum shear strain increment with elements at yield in tension obtained by constraining a factor of safety of unity. The inset shows the modelled groundwater flow net for the aquifer in the lower slide part. *Step 2*, **b** modelled change in groundwater pressure between high and low pressure states. **c** Modelled landslide state after 38 years of groundwater pressure changes. **d** Factor of safety for model elements during a high groundwater pressure state. White lines in **a**, **d**, and in the inset are water tables, i.e., level at which the water pressure is atmospheric

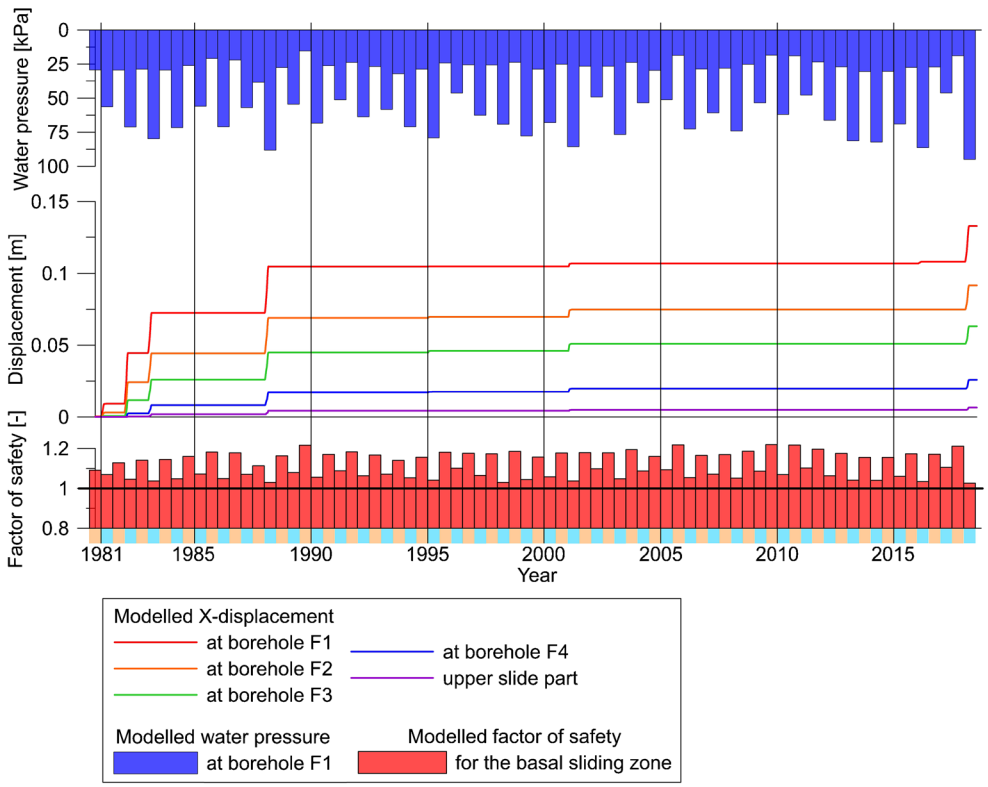

Fig. 5 *Step 2* (above) modelled groundwater pressure in borehole F1 (at 10-m depth), (middle) modelled displacement at boreholes F1, F2, F3, F4, and in the upper slide part, and (below) modelled factor of safety for the basal sliding zone, as a function of time. Refer to Fig. 3 for the location of observation points. Opaque orange and blue intervals below the time axis indicate the summer and winter periods, respectively

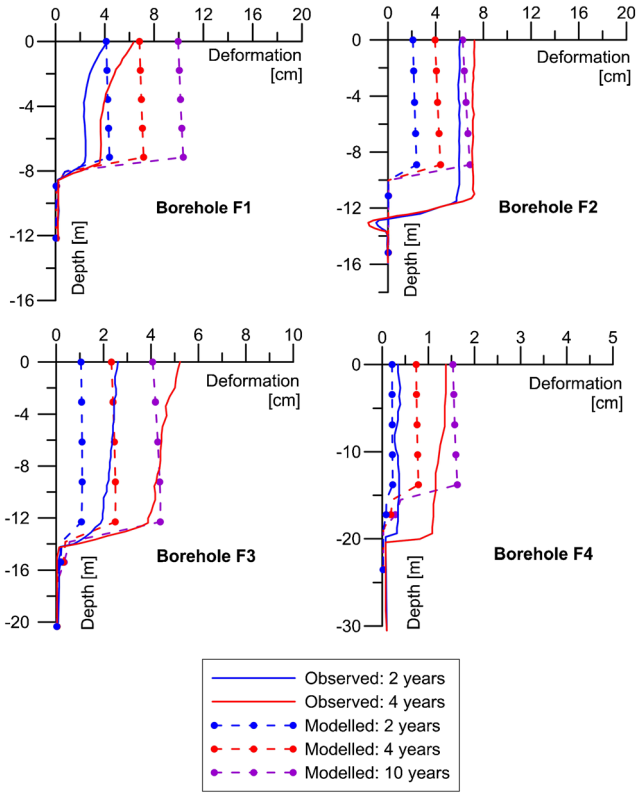

Fig. 6 *Step 2*, modelled against observed deformations as a function of depth in boreholes F1, F2, F3, and F4

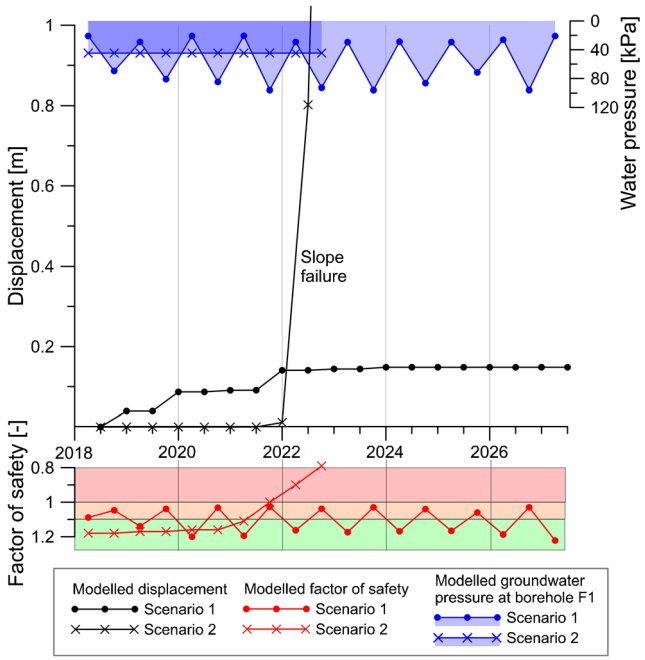

Fig. 7 *Step 3*, groundwater pressure changes, displacement in the lower slide part, and factor of safety for the two scenarios modelling possible failure mechanisms. Note that for scenario 1, the modelled factor of safety is the ratio between resisting and driving forces at the basal sliding zone, while for scenario 2 it considers all the landslide

(Fig. 4b) is the principal process modifying effective stresses in the slope and triggering the episodic movement (Fig. 4c). Movement may also accompany a loss of strength of the sliding mass. Figure 5 shows changes in groundwater pressure at the slide's toe, displacements, and the factor of safety (*FoS*) for the basal sliding zone as a function of time. During the winter period, the modelled increase in groundwater pressure in permeable layers of the perched aquifer causes a decrease of the shear strength of the basal sliding zone accompanied by movement reactivation with displacements of several centimeters in the lower slide part. There is satisfactory agreement between modelled and observed displacement at boreholes F1, F2, F3, F4, and in the upper part of Les Buges (Fig. 6). This validates parametric inputs for strain softening, i.e., mobilized and residual values, as well as the softening function, used for the sliding mass: c_{3k} limestones (Table 2). Figure 5 shows how the *FoS* comes closer to the unity in the winter period but remains positive. This is further illustrated in Fig. 4d showing the elemental *FoS*, i.e., ratio between resisting to driving forces for each element in the model, for a high (winter 2018) groundwater pressure state. Orange to purple colors stand for elements with $FoS > 1$, while red colors stand for elements with $FoS < 1$. It can be seen how the elemental *FoS* changes in the basal sliding zone, especially close to borehole F1, in response to the fluctuation of groundwater pressure in permeable layers at the slide's toe. During winter periods, if groundwater pressure is large enough, the lower slide body withstands only part of the driving forces with the re-activation of the episodic movement.

Step 3: long-term prediction of slide stability

Two possible failure mechanisms are tested for predicting slide activity in the long term. *Scenario 1* considers changing infiltration rates due to the effect of climate change. Climate scenarios for Western Switzerland anticipate a reduction of summer precipitation between − 32 and 0% and an increase of winter precipitation between 0 and + 21% by 2060 (CH2018 2018). These predictions are in line with field observations of recent years with long dry periods between summer and autumn and precipitation of high intensity in winter (Fig. 2a). According to these data, a recharge function respecting the aforementioned trends has been applied to the model for 10 years. Figure 7 illustrates obtained results. The modelled slope activity under climate change is in line with the behavior simulated during *Step 2* that is the slide will continue to move at slow rates controlled by groundwater pressure changes in the slope.

Scenario 2 models a progressive loss of shear strength of the sliding mass from mobilized to residual values. This mimics the increase of damage, especially in the lower slide part, due to internal distortion mechanisms characteristic for compound slides (Hungr et al. 2014; Preisig et al. 2016) and has been implemented in the model by a progressive reduction of cohesion of q_4 moraine deposits (SP-SM) from 0.1 to 0.01 MPa with a decrement of 0.01 per season. Figure 7 shows that the *FoS* of the modelled slide reaches the unity as the cohesion of the sliding mass is reduced to 0.03 MPa. Any further reduction leads to the failure of the lower slide part as illustrated in Fig. 7 by displacements becoming extremely high. Nevertheless, the modelled failure due to a progressive loss of strength of the sliding mass is focused at the slide's toe and does not trigger an ultimate failure affecting a large volume of the slide.

Discussion and conclusions

The one-way coupled hydromechanical procedure documented in this note is based on three steps targeting (*Step 1*) the calculation of strength properties and (*Step 2*) the verification of triggering phenomena for (*Step 3*) predicting the long-term activity of a deep-seated landslide. The method has been successfully applied for making predictions on the long-term activity of the *west body* of Les Buges compound slide in the Swiss Jura Mountains. Modelling results are in line with field observations suggesting that, under natural conditions, deep-seated compound slides rarely pick-up speed and evolve in an ultimate failure comprising a large volume of the slope. This is principally because the geometry, i.e., a sub-horizontal shear zone, and strength of the "stabilizing" lower slide part allow the slope to withstand (natural) triggering phenomena. According to Popescu (1994), deep-seated compound slides become thus in the long-term *actively unstable* slopes characterized by episodic movement but where natural effective stress changes and/or progressive loss of material strength of the sliding mass are insufficient to trigger an ultimate failure affecting a large part of the slope. This is in contrast with deep-seated collapse slides where the *actively unstable* state might evolve in the long term into an ultimate failure involving large volumes in response to a natural triggering process and/or the progressive loss of material strength (Hungr et al. 2014). The proposed modelling procedure is applicable if assumptions and limitations listed in Table 1 are respected. In such a case and if constrained by field data, the procedure is a reliable tool for assessing the long-term activity of deep-seated landslides and helping with their management.

This technical note is part of the *JuraHydroSlide* project, which aims to investigate hydrogeologic effects on landslides of the Swiss Jura Mountains and develop tools for making predictions on their activity. The present work focusses on the long-term behavior of deep-seated landslides. Future activities will look into other types of landslide phenomena occurring in the Jura Mountains via field studies and numerical modelling: rotational and planar shallow slides, debris flows and peat flows, as well as rock avalanches.

Acknowledgments

I gratefully acknowledge the referees for their comments and time spent to review this contribution, as well as Renato Macciotta for a careful review. This work was carried out within the framework of the *JuraHydroSlide* project sponsored by the Swiss National Science foundation (Project No. 184875).

References

CH2018 (2018) CH2018 – Climate scenarios for Switzerland, Technical Report. National Centre for Climate Services, Zurich 271pp

Crosta GB, Agliardi F (2003) Failure forecast for large rock slides by surface displacement measurements. Can Geotech J 40:176–191

Dawson EM, Roth WH, Drescher A (1999) Slope stability analysis by strength reduction. Géotechnique 49(6):835–840

De Boni M (2018) Etude hydrogéologique du glissement profond des Buges à Boudry (NE). MSc Thesis, Centre for Hydrogeology and Geothermics, University of Neuchâtel, Switzerland

Eberhardt E, Stead D, Coggan JS (2004) Numerical analysis of initiation and progressive failure in natural rock slopes – the 1991 Randa rockslide. Int J Rock Mech Min Sci 41(1):69–87

Eberhardt E, Preisig G, Gischig V (2016) Progressive failure in deep-seated rockslides due to seasonal fluctuations in pore pressures and rock mass fatigue. In: Experience, Theory and Practice, Aversa et al (eds) Landslides and engineered slopes. Associazione Geotecnica Italiana, Rome, pp 121–136

Fukuzono T (1985) A new method for predicting the failure time of a slope. In: Proceedings of the IVth International Conference and Field Workshop on Landslides. National Research Center for Disaster Prevention, Tokyo, pp 145–150

Gischig V, Preisig G, Eberhardt E (2016) Numerical investigation of seismically induced rock mass fatigue as a mechanism contributing to the progressive failure of deep-seated landslides. Rock Mech Rock Eng 49:2457–2478

Grämiger LM, Moore JR, Gischig VS, Ivy-Ochs S, Loew S (2017) Beyond debuttressing: mechanics of paraglacial rock slope damage during repeat glacial cycles. J Geophys Res Earth Surf 122(4):1004–1036

Hendry MT, Macciotta R, Martin DC, Reich B (2015) Effect of Thompson river elevation on velocity and instability of Ripley slide. Can Geotech J 52(3):257–267

Hungr O, Evans SG (2004) The occurrence and classification of massive rock slope failure. Felsbau, Vienna, Austria 22:16–23

Hungr O, Leroueil S, Picarelli L (2014) The Varnes classification of landslide types, an update. Landslides 11(2):167–194

Itasca (2018) FLAC 8.0 Fast Lagrangian Analysis of Continua - user guide. Itasca Consulting Group, Minneapolis

Kukemilks K, Wagner J-F, Saks T, Brunner P (2018) Physically based hydrogeological and slope stability modeling of the Turaida castle mound. Landslides 15(11):2267–2278

Lateltin O, Haennig C, Raetzo C, Bonnard C (2005) Landslide risk management in Switzerland. Landslides 2(4):313–320

Leonard GS, Gregg CE, Johnston DM (2013) Early warning systems. In: Bobrowsky P et al (eds) Encyclopedia of natural hazads. Springer Science+Business Media, Dordrecht, 1133pp

Leonarduzzi E, Molnar P, McArdell BW (2017) Predictive performance of rainfall thresholds for shallow landslides in Switzerland from gridded daily data. Water Resour Res 53(8):6612–6625

Leroueil S, Vaunat J, Picarelli L (1996) A geotechnical characterization of slope movements. Proceedings of the Seventh International Symposium on Landslides, Trondheim. A.A. Balkema, Rotterdam

Loew S, Gschwind S, Gischig V, Keller-Signer A, Valenti G (2017) Monitoring and early warning of the 2012 Preonzo catastrophic rockslope failure. Landslides 14(1):141–154

Meia J (1996) Gorges de l'Areuse. Glissement des Buges. Géologie. Rapport de synthèse sur l'étude 1977-1996. Technical report. Centre de documentation du service des ponts et chaussées, Neuchâtel

MeteoSwiss (2018) CLIMAP-net: portail de données météorologiques. Federal Office of Meteorology and Climatology MeteoSwiss, Geneva

Mike DHI (2018) Feflow 7.2 a flexible-mesh groundwater flow and transport simulation software - user guide. DHI WASY GmbH, Berlin

Pánek T, Klimeš J (2016) Temporal behavior of deep-seated gravitational slope deformations: A review. Earth-Science Reviews 156:14–38

Popescu (1994) A suggested method for reporting landslides causes. Bull Int Assoc Eng Geol 50:71–74

Preisig G (2018) Long-term effects of deep-seated landslides on transportation infrastructure: a case study from the Swiss Jura Mountains. QJEGH 52:326–335. https://doi.org/10.1144/qjegh2017-128

Preisig G, Eberhardt E, Smithyman M, Preh A, Bonzanigo L (2016) Hydromechanical rock mass fatigue in deep-seated landslides accompanying seasonal variations in pore pressures. Rock Mech Rock Eng 49:2333–2351

Routes Nationales Suisses (1996) N5 – rapport de synthèse géologique, hydrogéologique, géotechnique, km 29.940 à 31.480. Technical report. Archives of the Centre for hydrogeology and geothermics, University of Neuchâtel, Switzerland

Strozzi T, Delaloye R, Kääb A, Ambrosi C, Perruchoud E, Wegmüller U (2010) Combined observations of rock mass movements using satellite SAR interferometry, differential GPS, airborne digital photogrammetry, and airborne photography interpretation. J Geophys Res 115(F1):11pp

Tacher L, Bonnard C, Laloui L, Parriaux A (2005) Modelling the behaviour of a large landslide with respect to hydrogeological and geomechanical parameter heterogeneity. Landslides 2(1):3–14

Vuillet L, Hutter K (1988) Viscous-type sliding laws for landslides. Can Geotech J 25(3):467–477

G. Preisig (✉)
Centre for Hydrogeology and Geothermics,
University of Neuchâtel,
Emile-Argand 11, CH-2000, Neuchâtel, Switzerland
Email: giona.preisig@unine.ch